28 June 1999

PHYSICS LETTERS A

ELSEVIER

Physics Letters A 257 (1999) 153–157

A numerical study of the transition in the circular hydraulic jump

Kensuke Yokoi [a,b,c,1], Feng Xiao [a]

[a] *Computational Science Laboratory, The Institute of Physical and Chemical Research (RIKEN), Wako 351-0198, Japan*
[b] *Department of Mathematics, and Research Institute for Electronic Science, Hokkaido University, Sapporo 060-0812, Japan*
[c] *Department of Physics, Ibaraki University, Mito 310-8512, Japan*

Received 19 January 1999; received in revised form 19 April 1999; accepted 2 May 1999
Communicated by A.R. Bishop

Abstract

We performed axisymmetric (r-z) simulations to clarify the structure formation of the circular hydraulic jump. The transition from a type I to a type II jump, which was induced by changing the depth of the fluid far away from the jet in the laboratory experiment, was investigated numerically. We found that the transition is associated with a rise in pressure beneath the surface immediately after the hydraulic jump. This result shows that the hydrostatic assumption used in most of the theoretical studies may not be appropriate for the formation of a type II jump. © 1999 Elsevier Science B.V. All rights reserved.

PACS: 47.15.Cb; 83.20.Hn; 83.20.Jp; 83.50.Lh
Keywords: Hydraulic jumps; Numerical simulation; Free surface flow; Stratified flow

The schematic figure of a circular hydraulic jump is shown in Fig. 1(a). The vertical liquid jet impinges on the horizontal plate and spreads out radially, and the circular hydraulic jump is then formed. The phenomenon can also be observed in a kitchen sink and has been so far investigated experimentally and theoretically by many researchers [1–8].

In some experiments [6,8], the depth on the outside of the jump was controlled by varying the height of a circular wall d as shown in Fig. 1. Experimental results show that a circular hydraulic jump has two kinds of steady states that are reached by changing d [6]. When d is small or 0, a steady state with the eddy on the bottom is formed as in Fig. 1(a). This flow structure is called type I. On increasing d the jump becomes steep until a critical d_c is reached. If d becomes larger than d_c, the liquid outside the jump topples. Then, another steady state with not only the eddy on the bottom but also on the surface is formed as in Fig. 1(b). This flow structure is called type II and the eddy on the surface is called a roller. Recent experimental results show that the circular hydraulic jump can change into various regular polygonal shapes by changing d in type II [8].

In the theoretical studies, a rough scaling relation of the radius of the circular hydraulic jump has been proposed in [5]. This scaling relation is simple but agrees rather well with experimental data. A theoreti-

[1] E-mail: kensuke@atlas.riken.go.jp

PII: S0375-9601(99)00287-X

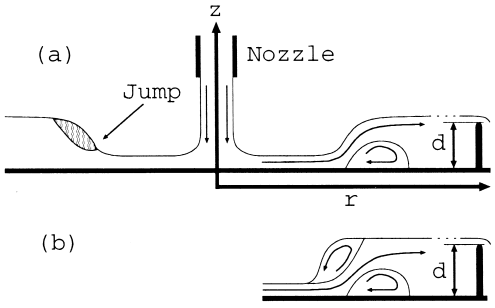

Fig. 1. Schematic figures of the circular hydraulic jump. The radius of the wall is much larger than the radius of the jump. The flow from the nozzle is constant. In the experiment, a high viscous liquid is used for controlling the instability of the flow pattern. (a) and (b) are called Type I and Type II respectively.

cal model has been developed for type I [7], but none for type II is available yet. In the theoretical studies, an hydrostatic pressure distribution in the vertical direction has been assumed for mathematical convenience, with no vertical variation of the pressure gradient. Such vertical variation may play an essential role in some cases, and an analysis that includes the non-hydrostatic effects appears necessary for understanding the mechanism of hydraulic jump problems.

Numerical simulation, which has proved a useful means for various fluid dynamic problems, has been also used for the hydraulic jump problem in [6], where a preset fixed boundary was used to represent the real free surface of the liquid. The simulation for the circular hydraulic jump is difficult due to the existence of a free boundary and the discontinuity along the liquid surface. In the present work, we performed numerical simulations based on a set of full fluid dynamic equations by using some recently developed numerical methods. Our simulation results show that the transition from type I to type II is associated with an increase in pressure beneath the surface in the region after the hydraulic jump (as indicated by the gray area in Fig. 1(a)). We believe that the pressure gradient yielded by the pressure increase has an important role for the transition.

In the present study, we made use of the C-CUP (CIP-Combined, Unified Procedure) method [9]. By using the C-CUP method, we are able to deal with both the gas and the liquid phases in an unified framework, and the explicit treatment of the free boundary and the interfacial discontinuity is not needed.

Here we briefly explain the numerical procedure. The liquid and the air obey the same hydrodynamic equations. The liquid and the gas are both assumed to have an equation of state in the form of a polytropic gas, but with quite different sound speeds. The sound speed is large for the liquid phase. The governing equations can be written as

$$\frac{\partial \rho}{\partial t} + (\boldsymbol{u}\cdot\nabla)\rho = -\rho\nabla\cdot\boldsymbol{u}, \tag{1}$$

$$\frac{\partial \boldsymbol{u}}{\partial t} + (\boldsymbol{u}\cdot\nabla)\boldsymbol{u} = -\frac{\nabla p}{\rho} + \boldsymbol{g} + \nu\Delta\boldsymbol{u} + \sigma\kappa\frac{\nabla\phi}{\rho}, \tag{2}$$

$$\frac{\partial p}{\partial t} + (\boldsymbol{u}\cdot\nabla)p = -\gamma p\nabla\cdot\boldsymbol{u}, \tag{3}$$

$$\frac{\partial \phi}{\partial t} + (\boldsymbol{u}\cdot\nabla)\phi = 0, \tag{4}$$

where ρ is the density, $\boldsymbol{u}$ the velocity, p the pressure, $\boldsymbol{g}$ the gravitational acceleration, ν the kinematic viscosity, σ the liquid surface tension coefficient, κ the curvature, ϕ the density function and γ the specific heat ratio. We use the CSF (Continuum Surface Force) model [10] to evaluate surface tension. The density function is defined to distinguish different materials [11].

An axis-symmetric model has been constructed to deal with the circular hydraulic jump. The configuration of the simulation model on an r-z plane is shown in Fig. 2.

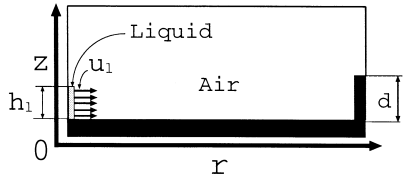

Fig. 2. Schematic figure for the initial condition of the simulation. The dark part indicates the no-slip wall. The liquid is jetted from the lower left to the right direction with a speed u_1. A 200×60 Cartesian grid with $\Delta r = \Delta z = 0.1$ mm is used.

As a validation of the present computational model, we compared the radius of the simulation results with the scaling relation [5]

$$r_j \sim q^{5/8} \nu^{-3/8} g^{-1/8}, \tag{5}$$

here r_j is the radius of the jump, $q = Q/2\pi$ and Q is the volume flux ($2\pi ruh$ with h being the depth of the liquid). In the present study, the jump is identified as the position where $\partial h/\partial r$ has its maximum. Fig. 3 shows the jump radius of the simulation results and the scaling relation as a function of q (a) and the kinematic viscosity (b). Consistent with the scaling relation, the computational model gives a reasonable response to the different physical parameters. As expected from the scaling relation, the jump radius becomes larger based on a $r_j \sim q^{5/8}$ law if the inflow flux is increased, while the jump radius declines in a $r_j \sim \nu^{-3/8}$ law as the viscosity increases. As can be seen from the scaling relation, the jump radius depends on the volume flux rather than the mass flux. It means that the density of the liquid plays no role in determining the jump radius. This observation is confirmed by running simulations with different liquid density ρ_l. The results for different ρ_l are also plotted in Fig. 3(a). No significant influence from ρ_l on the jump radius is found.

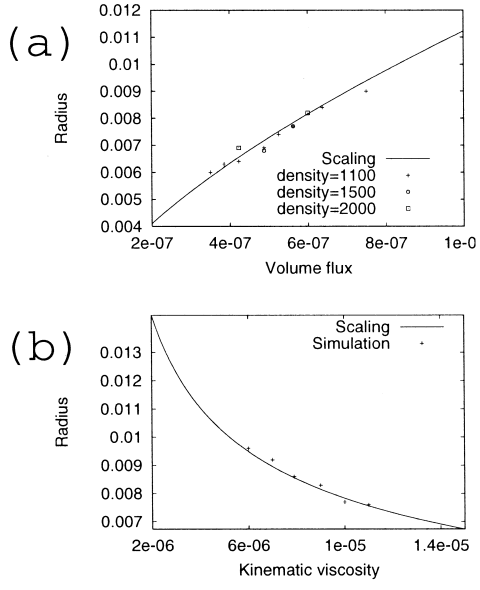

Fig. 3. The jump radii of the simulation results were plotted as a function of the volume flux (a) and the kinematic viscosity (b). The conditions as $d = 0$ mm, $h_l = 1.3$ mm and $u_l = 1.5$ m/s were set for all cases. In (a) $\nu = 1.0\times10^{-5}$ m^2/s and several values were specified for the liquid density ρ_l (1100 kg/m^3, 1500 kg/m^3 and 2000 kg/m^3). A volume flux $q = 5.625\times10^{-7}$ m^3/s and the liquid density $\rho_l = 1100$ kg/m^3 were used for (b). Symbols and the solid line represent the jump radii of the simulation results and of the scaling relation.

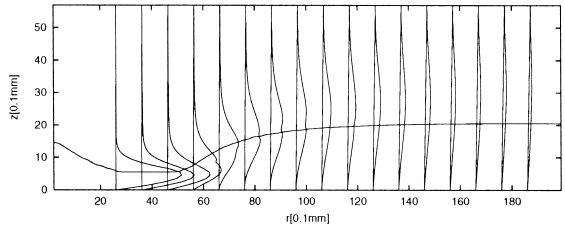

Fig. 4. The surface and the horizontal velocity profiles of a type I jump. $\rho_l = 1100$ kg/m^3, $\nu_l = 1.0\times10^{-5}$ m^2/s, $\rho_a = 10$ kg/m^3, $\sigma = 4.5\times10^{-2}$ N/m, $d = 0.3$ mm, $h_l = 1.5$ mm and $u_l = 2.0$ m/s are used.

As examples of the formation of type I and type II jumps, we performed simulations with $\sigma = 4.5\times10^{-2}$ N/m, using different wall heights d. Fig. 4 shows the steady state of a type I jump with $d = 0.3$ mm. Fig. 5 shows the time evolution for the formation of a type II jump with $d = 0.7$ mm. We found from our calculations that a type I jump usually forms when $d \le 0.4$ mm, while a type II jump develops if d is larger than 0.5 mm as d increases from 0.

The pressure distributions after eliminating the hydrostatic effect for the steady state of a type I jump (Fig. 4) and the state immediately before the transition to a type II jump (Fig. 5 at $t = 0.95$ s) were plotted in Fig. 6. It is observed that there is an increase in pressure immediately after the jump. The development of the high pressure region may be attributed to the interaction between the surface tension and the main flow current turned up toward the surface. The surface tension suppresses the flow from below and causes a rise in pressure. This increase in pressure needs to balance the surface tension and the driving flow to produce a steady jump. As a result of the pressure increase, a pressure gradient in the horizontal direction, which tends to cause a reverse flow, is formed beneath the surface. In the case that a type II jump is formed, the pressure gradient is larger than that in the case of a type I jump. When this pressure gradient becomes stronger

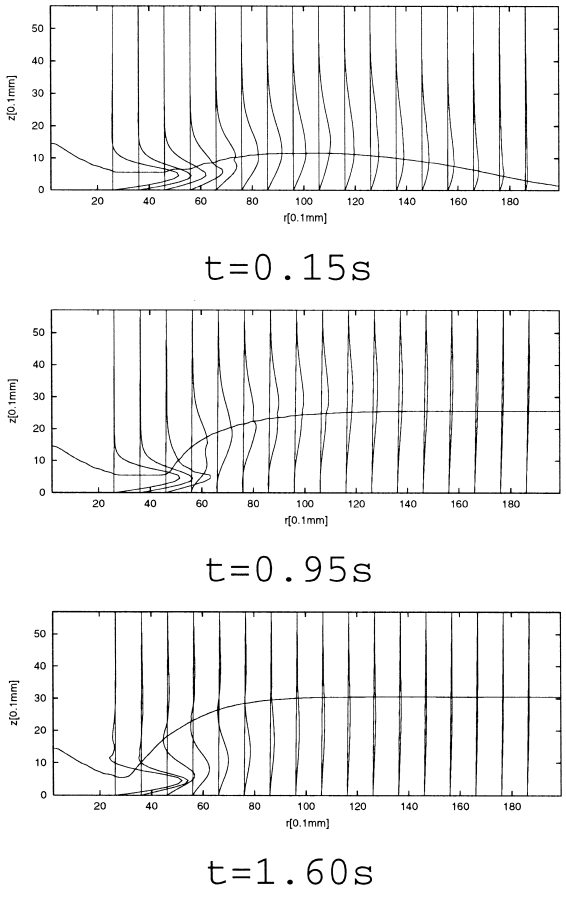

Fig. 5. The time evolution for the formation of a type II jump with $d = 0.7$ mm.

than the flow from below, a roller is created. From the above discussion, we may conclude that the establishment of a high pressure near the jump should be essential for the formation of a type II jump. The competition between the reverse pressure gradient

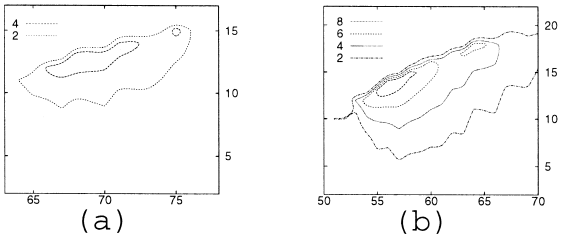

Fig. 6. The hydrostatic effect free pressure [Pa] contours around the jump of Fig. 4(a) and Fig. 5(b) at $t = 0.95$ s.

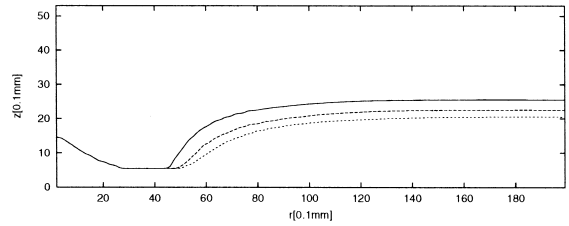

Fig. 7. Surface profiles for varying d. The jumps of type I of $d = 0.3$ mm, $d = 0.4$ mm and $d = 0.5$ mm were plotted. The maximum values of hydrostatic effect free pressure around the jumps were 9.0 Pa, 10.6 Pa and 12.6 Pa, respectively.

force and the driving flow determines the occurrence of the roller.

The transition from type I to type II by increasing d can be explained by the occurrence of the pressure increase. From the experimental results [6] and our simulation results (Fig. 7), it can be known that a steeper jump is always associated with a higher wall height d in a type I jump. Thus, as d is increased, the curvature of the interface in the region immediately after the jump becomes larger, then the surface tension is strengthened, because the surface tension is proportional to the curvature. In order to counteract this surface tension and keep the jump surface steady, a larger rise in pressure is required. To confirm this, we measured the largest pressure around the jump for different d. For the higher wall height d in a type I jump, the higher pressure was observed (Fig. 7). As a result of heightening d in a type I jump, a stronger pressure gradient is established. If d is increased over d_c, the reverse pressure gradient becomes stronger than the flow from below and a roller occurs.

In summary, axis-symmetrical simulations were carried out for the circular hydraulic jump. The transition from type I to type II was reproduced by changing d. We found that a type II jump formation depends on the establishment of a high pressure region after the jump.

Acknowledgements

We would like to thank S. Watanabe (Ibaraki University), H. Nishimori (Osaka Prefecture University), T. Ebisuzaki and K. Sunouchi (RIKEN) for

important suggestions and discussions. Numerical computation in this work was partially carried out at the Computer Information Center, RIKEN and the Yukawa Institute for Theoretical Physics, Kyoto University. K.Y. is grateful to RIKEN for a JRA fellowship.

References

[1] Lord Rayleigh, Proc. Roy. Soc. London A 90 (1914) 324.
[2] I. Tani, J. Phys. Soc. Jpn. 4 (1949) 212.
[3] E.J. Watson, J. Fluid. Mech. 20 (1964) 481.
[4] A.D.D. Craik, R.C. Latham, M.J. Fawkes, P.W.F. Gribbon, J. Fluid. Mech. 112 (1981) 347.
[5] T. Bohr, P. Dimon, V. Putkaradze, J. Fluid. Mech. 254 (1993) 635.
[6] T. Bohr, C. Ellegaard, A.E. Hansen, A. Haaning, Physica B 228 (1996) 1.
[7] T. Bohr, V. Putkaradze, S. Watanabe, Phys. Rev. Lett. 79 (1997) 1038.
[8] C. Ellegaard, A.E. Hansen, A. Haaning, K. Hansen, A. Marcussen, T. Bohr, J.L. Hansen, S. Watanabe, Nature 392 (1998) 767.
[9] T. Yabe, P.Y. Wang, J. Phy. Soc. Jpn. 60 (1991) 2105.
[10] J.U. Brackbill, D.B. Kothe, C. Zemach, J. Comp. Phys. 100 (1992) 335.
[11] T. Yabe, F. Xiao, J. Phy. Soc. Jpn. 62 (1993) 2537.